Springer

Journal of
Mechanical
Science and
Technology

Journal of Mechanical Science and Technology 23 (2009) 2635~2644

www.springerlink.com/content/1738-494x
DOI 10.1007/s12206-009-0716-6

Nonlinear transient heat transfer and thermoelastic analysis of thick-walled FGM cylinder with temperature-dependent material properties using Hermitian transfinite element †

Mohammad Azadi[1,*] and Mahboobeh Azadi[2]

[1]*Department of Mechanical Engineering, Sharif University of Technology, Azadi St., Tehran, Iran*
[2]*Department of Material Engineering, Shiraz University, Namazi Sq., Shiraz, Iran*

(Manuscript Received May 19, 2008; Revised May 13, 2009; Accepted May 25, 2009)

Abstract

Nonlinear transient heat transfer and thermoelastic stress analyses of a thick-walled FGM cylinder with temperature-dependent materials are performed by using the Hermitian transfinite element method. Temperature-dependency of the material properties has not been taken into account in transient thermoelastic analysis, so far. Due to the mentioned dependency, the resulting governing FEM equations of transient heat transfer are highly nonlinear. Furthermore, in all finite element analysis performed so far in the field, Lagrangian elements have been used. To avoid an artificial local heat source at the mutual boundaries of the elements, Hermitian elements are used instead in the present research. Another novelty of the present paper is simultaneous use of the transfinite element method and updating technique. Time variations of the temperature, displacements, and stresses are obtained through a numerical Laplace inversion. Finally, results obtained considering the temperature-dependency of the material properties are compared with those derived based on temperature independency assumption. Furthermore, the temperature distribution and the radial and circumferential stresses are investigated versus time, geometrical parameters and index of power law. Results reveal that the temperature-dependency effect is significant.

Keywords: Transfinite element; Thermoelastic stresses; Transient heat transfer; FGM; Temperature-dependency; Nonlinear analysis; Thick-walled cylinder; Numerical Laplace inversion

1. Introduction

FGM components are generally constructed to sustain elevated temperatures and severe temperature gradients. Low thermal conductivity, low coefficient of thermal expansion and core ductility have enabled the FGM material to withstand higher temperature gradients for a given heat flux. Examples of structures that undergo extremely high temperature gradients are plasma facing materials, propulsion system of planes, cutting tools, engine exhaust liners, aerospace skin structures, incinerator linings, thermal barrier coatings of turbine blades, thermal resistant tiles, and directional heat flux materials. Continuously varying the volume fraction of the mixture in the FGM materials eliminates the interface problems and mitigates thermal stress concentrations and causes a more smooth stress distribution.

Extensive thermal stress studies made by Noda [1] reveal that the weakness of the fiber-reinforced laminated composite materials, such as delamination, huge residual stress, and locally large plastic deformations, may be avoided or reduced in FGM materials. Tanigawa [2] presented an extensive review that covered a wide range of topics from thermoelastic to thermo-inelastic problems. He compiled a compre-

† This paper was recommended for publication in revised form by Associate Editor Jeonghoon Yoo
*Corresponding author. Tel.: +98 21 2220 1301, Fax.: +98 21 2220 1301
E-mail address: azadi@mech.sharif.ir

hensive list of papers on the analytical models of thermoelastic behavior of FGM. The analytical solution for the stresses of FGM in the one-dimensional case for spheres and cylinders are given by Lutz and Zimmerman [3, 4]. These authors consider the non-homogeneous material properties as linear functions of radius. Obata et al. [5] presented the solution for thermal stresses of a thick hollow cylinder, under a two-dimensional transient temperature distribution, made of FGM. Sutradhar et al. [6] presented a Laplace transform Galerkin BEM for 3-D transient heat conduction analysis by using the Green's function approach where an exponential law for the FGMs was used. Kim and Noda [7] studied the unsteady-state thermal stress of FGM circular hollow cylinders by using Green's function method. Reddy and co-workers [8-13] carried out theoretical as well as finite element analyses of the thermo-mechanical behavior of FGM cylinders, plates and shells. Geometric non-linearity and the effect of coupling item were considered for different thermal loading conditions. Shao and Wang [14-16] studied the thermo-mechanical stresses of FGM hollow cylinders and cylindrical panels with the assumption that the material properties of FGM followed simple laws, e.g., exponential law, power law or mixture law in thickness direction. An approximate static solution of FGM hollow cylinders with finite length was obtained by using a multi-layered method; analytical solution of FGM cylindrical panel was carried out by using the Frobinus method; and analytical solution of transient thermo-mechanical stresses of FGM hollow cylinders were derived by using the Laplace transform technique and the power series method, in which effects of material gradient and heat transfer coefficient on time-dependent thermal mechanical stresses were discussed in detail. Similarly, Ootao and Tanigawa [17-19] obtained the analytical solutions of unsteady-state thermal stress of FGM plate and cylindrical panel due to non-uniform heat supply. Using the multi-layered method and through a novel limiting process, Liew and et al. [20] obtained analytical solutions of steady-state thermal stress in FGM hollow circular cylinder. Using finite difference method, Awaji and Sivakuman [21] studied the transient thermal stresses of an FGM hollow circular cylinder, which is cooled by the surrounding medium. Ching and Yen [22] evaluated the transient thermoelastic deformations of 2-D functionally graded beams under non-uniformly convective heat supply.

In this paper, by using the Hermitian transfinite element method, nonlinear transient heat transfer and thermoelastic stress analyses are performed for thick-walled FGM cylinder, which materials are temperature-dependent. Time variations of the temperature, displacements, and stresses are obtained through a numerical Laplace inversion. Finally, results are obtained considering the temperature-dependency of the material properties. Those results are the temperature distributions and the radial and circumferential stresses are investigated versus time, geometrical parameters and index of power law (N) and then they are compared with those derived based on the temperature independency assumption.

Two main novelties of this research are incorporating the temperature-dependency of the material properties and proposing a numerical transfinite element procedure that may be used in the Picard iterative algorithm to update the material properties in a highly nonlinear formulation. In contrast to earlier researches, second order elements are employed. Therefore, the proposed transfinite element method may be adequately used in problems where the time integration method is not recommended because of truncation errors (e.g., coupled thermo-elasticity problems with very small relaxation times) or where improper choice of time integration step may lead to loss of the higher frequencies in the dynamic response. Also, the accumulated errors that are common in the time integration method and in many cases lead to remarkable errors, numerical oscillations, or instability, do not happen in this technique.

2. The governing equations

Geometric parameters of the thick-walled FGM cylinder are shown in Fig. 1. The FGM cylinder is assumed to be made of a mixture of two constituent materials so that the inner layer of the cylinder is ce-

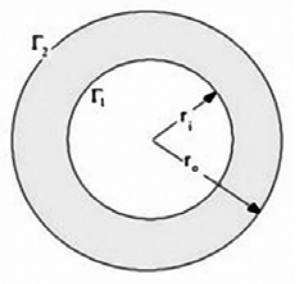

Fig. 1. FGM thick-walled cylinder.

ramic-rich, whereas the external surface is metal-rich.

The properties can be expressed as follows:

$$P = P_0(P_{-1}T^{-1} + 1 + P_1T + P_2T^2 + P_3T^3) \quad (1)$$

Where P_0, P_{-1}, P_1, P_2 and P_3 are constants in the cubic fit of the materials' property. The materials' properties are expressed in this way so that higher order effects of the temperature on the material properties can be readily discernible. Volume fraction is a spatial function, whereas the properties of the constituents are functions of temperature. The combination of these functions gives rise to the effective material properties of FGM and can be expressed by

$$P_{eff}(T, r) = P_m(T)V_m(r) + P_c(T)V_c(r) \quad (2)$$

Where P_{eff} is the effective material property of FGM, and P_m and P_c are the temperature dependent properties metal and ceramic, respectively. V_c is the volume fraction of the ceramic constituent of the FGM can be written by

$$V_c = \left(\frac{r_o - r}{r_o - r_i}\right)^N, \quad V_m = 1 - V_c \quad (3)$$

Where volume fraction index N dictates the material variation profile through the beam thickness and may be varied to obtain the optimum distribution of component materials ($0 \leq N \leq \infty$). From the above equation, the effective Young's modulus E, Poisson ratio v, thermal expansion coefficient α and mass density ρ of an FGM cylinder can be written by

$$P_{eff} = (P_c - P_m)\left(\frac{r_o - r}{r_o - r_i}\right)^N + P_m \quad (4)$$

In this paper, only the effective Young's modulus and thermal expansion coefficient are dependent on temperature. The related equation is

$$\begin{aligned} P = {} & P_{0c}(P_{-1c}T^{-1} + 1 + P_{1c}T + P_{2c}T^2 + P_{3c}T^3)V_c \\ & + P_{0m}(P_{-1m}T^{-1} + 1 + P_{1m}T + P_{2m}T^2 + P_{3m}T^3)V_m \end{aligned} \quad (5)$$

3. Finite element method

The equation of heat transfer is

$$-\frac{1}{r}\left[\frac{\partial T}{\partial r}\frac{\partial(\kappa r)}{\partial r} + \kappa r\frac{\partial^2 T}{\partial r^2}\right] + \rho C_v\frac{\partial T}{\partial t} = 0 \quad (6)$$

The boundary conditions are the heat flux in the internal layer and convection condition for external layer of FGM cylinder

$$\begin{cases} 2\pi\kappa r\dfrac{\partial T}{\partial r} + 2\pi rh(T - T\infty) = 0 & at\ r = r_o \\ -\kappa\dfrac{\partial T}{\partial r} = q_0 & at\ r = r_i \end{cases} \quad (7)$$

The initial condition is $T(t=0)=T_\infty$. Kantorovich approximation is

$$\{T(r,t)\} = [\tilde{N}(r)]\{T^{(e)}(t)\} \quad (8)$$

$[\tilde{N}]$ is the shape function matrix. For second order elements (with 3 nodes) which are used in temperature field:

$$[\tilde{N}] = \left[\frac{1}{2}\xi(\xi - 1)\ \ (1 - \xi^2)\ \ \frac{1}{2}\xi(\xi + 1)\right] \quad (9)$$

ξ, natural coordinate which changes between -1 and 1 is used because of the Gauss-Legendre numerical integration method. The relation between global and natural coordinate is

$$[\tilde{N}]_r = [\tilde{N}]_\xi \xi_r = [\tilde{N}]_\xi \frac{\Delta\xi}{\Delta r} = [\tilde{N}]_\xi \frac{2n}{r_o - r_i} \quad (10)$$

Where n is the number of elements. Residual integration form in Galerkin method is

$$\int_\Omega [\tilde{N}]^T R d\Omega = 0 \quad (11)$$

For a heat transfer problem, R is

$$\begin{aligned} R = {} & \rho c[\tilde{N}]\{\dot{T}^{(e)}\} - \\ & \frac{1}{r}\left[[\tilde{N}]_r\frac{\partial(\kappa r)}{\partial r} + \kappa r[\tilde{N}]_{rr}\right]\{T^{(e)}\} \end{aligned} \quad (12)$$

Then the heat transfer problem can be written by

$$[C^{(e)}]\{\dot{T}^{(e)}\} + [A^{(e)}]\{T^{(e)}\} = \{q^{(e)}\} \quad (13)$$

Matrices C, A and q are damping and stiffness matrices and force vector, respectively.

$$[C^{(e)}] = \int_\Omega [\tilde{N}]^T \rho c[\tilde{N}] d\Omega \quad (14a)$$

$$[A^{(e)}] = -\int_{\Omega}[\tilde{N}]^T \frac{1}{r}\frac{\partial(\kappa r)}{\partial r}[\tilde{N}]_r d\Omega + \int_{\Omega}[[\tilde{N}]^T{}_r \kappa + [\tilde{N}]^T \kappa_r][\tilde{N}]_r d\Omega + \int_{\Gamma_2}[\tilde{N}]^T h[\tilde{N}]d\Gamma_2 \quad (14b)$$

$$\{q^{(e)}\} = \int_{\Gamma}[\tilde{N}]^T \kappa \frac{\partial T}{\partial r}\cdot n_r \, d\Gamma = \int_{\Gamma_1}[\tilde{N}]^T q_0 d\Gamma_1 + \int_{\Gamma_2}[\tilde{N}]^T hT_{\infty} d\Gamma_2 \quad (14c)$$

Strain can be written as below:

$$\{\varepsilon\} = [d]\{u\} \quad (15)$$

$$\{\varepsilon\}^T = <\varepsilon_r \ \varepsilon_\theta>, \ [d]^T = \begin{bmatrix} \frac{\partial}{\partial r} & \frac{1}{r} \end{bmatrix} \quad (16)$$

Energy function is

$$\pi = \frac{1}{2}\int_{\Omega}\{\varepsilon\}^T\{\sigma\}d\Omega + \int_{\Omega}\rho\{u\}^T\{\ddot{u}\}d\Omega - \int_{\Gamma}\{u\}^T\{\hat{p}\}d\Gamma \quad (17)$$

And so

$$\delta\pi = \int_{\Omega}\delta(\{\varepsilon\}^T)\cdot\{\sigma\}d\Omega + \int_{\Omega}\rho\cdot\delta(\{u\}^T)\cdot\{\ddot{u}\}d\Omega - \int_{\Gamma}\delta(\{u\}^T)\cdot\{\hat{p}\}d\Gamma = 0 \quad (18)$$

Differential of strain is

$$\delta(\{\varepsilon\}^T) = \delta(\{u\}^T)\cdot[d]^T \quad (19)$$

Displacements in order to shape functions are

$$\{u\} = [N]\{U^{(e)}\} \quad (20)$$

[N] for displacement is a Hermitian shape function.

$$[N] = [N_1 \ \ \bar{N}_1 \ \ N_2 \ \ \bar{N}_2] \quad (21a)$$

$$N_1 = \frac{1}{4}(\xi-1)^2(2+\xi) \quad (21b)$$

$$\bar{N}_1 = \frac{1}{4}(1-\xi)^2(\xi+1) \quad (21c)$$

$$N_2 = \frac{1}{4}(\xi+1)^2(2-\xi) \quad (21d)$$

$$\bar{N}_2 = \frac{1}{4}(1+\xi)^2(\xi-1) \quad (21e)$$

And displacement vector is

$$\{U^{(e)}\}^T = \langle u_0^{(1)} \ u_0'^{(1)} \ u_0^{(2)} \ u_0'^{(2)}\rangle \quad (22)$$

By definition of

$$[B] = [d][N] \quad (23)$$

In which

$$[B] = \begin{bmatrix} N_{1r} & \bar{N}_{1r} & N_{2r} & \bar{N}_{2r} \\ \frac{N_1}{r} & \frac{\bar{N}_1}{r} & \frac{N_2}{r} & \frac{\bar{N}_2}{r} \end{bmatrix} \quad (24)$$

And then, Eq. (18) is changed to

$$\delta\pi = \int_{\Omega}\delta(\{U^{(e)}\}^T)[B]^T\cdot\{\sigma\}d\Omega + \int_{\Omega}\rho\cdot\delta(\{U^{(e)}\}^T)[N]^T\cdot\{\ddot{u}\}d\Omega - \int_{\Gamma}\delta(\{U^{(e)}\}^T)[N]^T\cdot\{\hat{p}\}d\Gamma \quad (25)$$

And it is simplified to

$$\int_{\Omega}[B]^T\cdot\{\sigma\}d\Omega + \int_{\Omega}\rho[N]^T\{\ddot{u}\}d\Omega - \int_{\Gamma}[N]^T\cdot\{\hat{p}\}d\Gamma = 0 \quad (26)$$

The relation between stress and strain is

$$\{\sigma\} = [D](\{\varepsilon\} - \{\varepsilon_T\}) \quad (27)$$

In which

$$\{\varepsilon_T\}^T = \langle \alpha\Delta T \ \ \alpha\Delta T\rangle \quad (28a)$$

$$[D] = \frac{E(r)}{1-\nu(r)^2}\begin{bmatrix} 1 & \nu(r) \\ \nu(r) & 1 \end{bmatrix} \quad (28b)$$

Then Eq. (26) becomes

$$\int_A\left([B]^T[D]([B]\{U^{(e)}\} - \{\varepsilon_T\}\right)dA + \int_A\rho[N]^T[N]\{\ddot{U}^{(e)}\}dA - \int_s[N]^T\cdot\{\hat{p}\}ds = 0 \quad (29)$$

A thermoelastic stress problem can be written as below:

$$[M^{(e)}]\{\ddot{\Phi}^{(e)}\}+[K^{(e)}]\{\Phi^{(e)}\}=\{f^{(e)}\} \tag{30}$$

Matrices M, K and f are mass and stiffness matrices and force vector, respectively.

$$[M^{(e)}]=\int_A \rho[N]^T[N]dA \tag{31a}$$

$$[K^{(e)}]=\int_A [B]^T[D][B]dA \tag{31b}$$

$$\{f^{(e)}\}=\int_A [N]^T\cdot\{\hat{p}\}dA+\int_A [B]^T[D]\{\varepsilon_T\}dA \tag{31c}$$

The general integral is

$$\begin{aligned}\int_\Omega L(r,\xi)d\Omega &= \int 2\pi r L(r,\xi)dr \\ &= 2\pi\int_{-1}^{1} rL(r,\xi)\frac{\Delta r}{\Delta\xi}dz \\ &= \pi\int_{-1}^{1} rL(r,\xi)\frac{r_o-r_i}{n}dz\end{aligned} \tag{32}$$

To solve the above equations, a program which writes in MATLAB is used.

Table 1. Geometrical characteristics.

Characteristic	Amount
Heat Flux (q_0)	1000 (kw/m^2)
Coefficient of Conduction (h)	8 (W/m^2·g)
Internal Radius (r_i)	12.7 (mm)
External Radius (r_o)	25.4 (mm)

Table 2. Coefficients of properties of FGM material.

Characteristics	Metal (Ti-6Al-4V)	Ceramic (Si_3N_4)
ρ (kg/m^2)	2370	4429
C_v(j/kgK)	625.29692	555.11
κ (W/mK)	13.723	1.20947
E(Gpa)	122.55676	348.43
ν	0.29	0.24
α (1/K)	7.5787 e -6	5.8723 e -6
$P_{-1}(E, \alpha)$	0	0
$P_1(E)$	-4.58635 e -4	-0.00037
$P_2(E)$	0	2.16 e -7
$P_3(E)$	0	-8.948 e -11
$P_1(\alpha)$	0.00065	9.095 e -4
$P_2(\alpha)$	0.313467 e -6	0
$P_3(\alpha)$	0	0

The geometrical characteristics and coefficients of properties of FGM cylinder are listed in Tables 1 and 2.

4. Laplace transform

Making application of the Laplace transform, defined by

$$\Omega(s)=L[\omega(t)]=\int_0^\infty e^{-st}\omega(t)dt \tag{33}$$

The governing equations become

$$(s[C^{(e)}]+[A^{(e)}])\{T(s)^{(e)}\}=\{Q(s)^{(e)}\} \tag{34}$$

$$(s^2[M^{(e)}]+[K^{(e)}])\{U(s)^{(e)}\}=\{F(s)^{(e)}\} \tag{35}$$

5. Numerical laplace inversion

To obtain the distributions of the displacement and temperature in the physical domain, it is necessary to perform Laplace inversion for the transformed displacement and temperature obtained when a sequence of values of s is specified. In this paper an accurate and efficient numerical method is used to obtain the inversion of the Laplace transform.

The inversion of the Laplace transform is defined as

$$\omega(t)=L^{-1}[\Omega(s)]=\frac{1}{2\pi i}\int_{v-i\infty}^{v+i\infty} e^{st}\Omega(s)ds \tag{36}$$

The numerical inversion of the Laplace transform can be written

$$\omega_N(t)=\frac{1}{2}\lambda_0+\sum_{k=1}^{p}\lambda_k \tag{37}$$

$$\begin{aligned}\lambda_k &= \frac{e^{-vt}}{T}\left\{\mathrm{Re}\left[\Omega\left(v+i\frac{k\pi}{T}\right)\right]\cos\frac{k\pi}{T}t\right\} \\ &-\frac{e^{-vt}}{T}\left\{\mathrm{Im}\left[\Omega\left(v+i\frac{k\pi}{T}\right)\right]\sin\frac{k\pi}{T}t\right\}\end{aligned} \tag{38}$$

It should be noted that a good choice of the free parameters p and vT is not only important for the accuracy of the results but also for the application of the Korrektur method [23] and the methods for the acceleration of convergence. The values of v and T are chosen according to the criteria outlined by Honig and Hirdes in [23].

After choosing the optimal *v*, any nodal variables in physical domain can be calculated at any specific instant by using the Korrektur method and e-algorithm simultaneously to perform the numerical Laplace inversion [23].

6. Numerical results

6.1 Results for temperature distribution

Here are the dimensionless parameters which are used in numerical results

$$R=\frac{r-r_i}{r_o-r_i},\ \bar{R}=\frac{r_o}{r_i},\ \bar{t}=\frac{t}{T} \tag{39}$$

Results obtained in Fig. 2 for different number of elements (n) shows that the results are convergent in $\bar{t}=0.5$. Hence, seven second-order elements are chosen to perform the next analyses.

The distribution of temperature is drawn for N=1 in Fig. 3. As expected, results of the consecutive times are convergent to each other and then the transient response vanishes and the steady-state response becomes the dominant.

Effect of index of power law for $\bar{t}=0.5$ is conducted in Fig. 4. As the volume fraction index increases, the volume fraction of the ceramic material increases in the vicinity of the hot boundary surface (the inner surface). Therefore, higher temperatures, and subsequently, higher temperature gradients are achieved in the neighborhood of the inner surface of the FGM cylinder. Furthermore, in this case, the temperature has converged asymptotically to the ambient temperature, at a higher rate.

Then, Fig. 5 shows the effect of change in geometry ($\bar{R}=r_o/r_i$) such as changing in internal and external radius, for $\bar{t}=0.5$ and N=1. Temperatures of the thinner cylinders are generally higher. Therefore, temperature distribution with lower temperature gradient is constructed. In other words, for thinner cylinders, the response is more convergent to the steady-state one.

Influence of temperature-dependency on temperature distribution of FGM cylinder is drawn in Fig. 6 for N=1, $\bar{t}=0.2$ and $\bar{R}=2$. This result shows that higher temperatures and temperature gradients result when the temperature-dependency of the material properties is ignored. A difference up to 15 percent in temperature is observed. Since according to Fig. 3, temperature values increase with the time, this difference is more remarkable for greater values of the dimensionless time ($\bar{t}$).

6.2 Results for thermoelastic stresses

Figs. 7 and 8 show radial and hoop stresses versus *R* and time for N=1. This result shows that radial and hoop stresses are increasing by time. In the inner layers of cylinder, stresses are higher because of higher temperature gradient. At both ends of the cylinder (inner and outer layers) radial stress is to some extent zero (according to the numerical errors in FEM) due to free surface and having no pressure.

For various index of power law (N), radial and hoop stresses are drawn in Figs. 9 and 10 for $\bar{t}=0.4$. By increasing of N, as FGM material becomes softer, both radial and hoop stresses are reduced.

Figs. 11 and 12 are shown for differences between dependency and independency of properties in temperature and then the changes in radial and hoop stresses for $\bar{t}=0.4$ and N=1. This result shows that higher stresses result when the temperature-dependency of material properties is ignored. A difference of up to 15 percent in stresses is observed. Since temperature values increase with the time (Fig. 3), stresses increase also (Fig. 7) and therefore this difference will be more remarkable for greater values of the dimensionless time ($\bar{t}$).

Geometry effect is shown in Figs. 13 and 14 for both radial and hoop stress. By increasing of thickness, stresses decrease due to decreasing of temperature gradient.

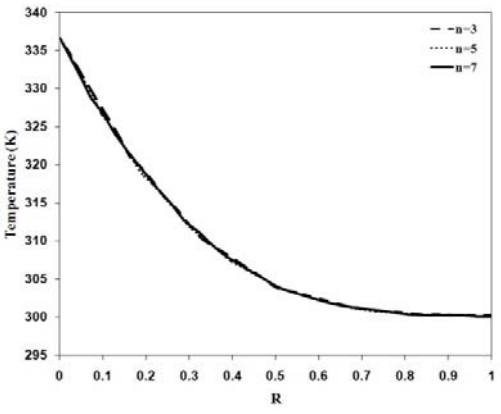

Fig. 2. Effect of element number on response of temperature for N=1 and $\bar{t}=0.5$.

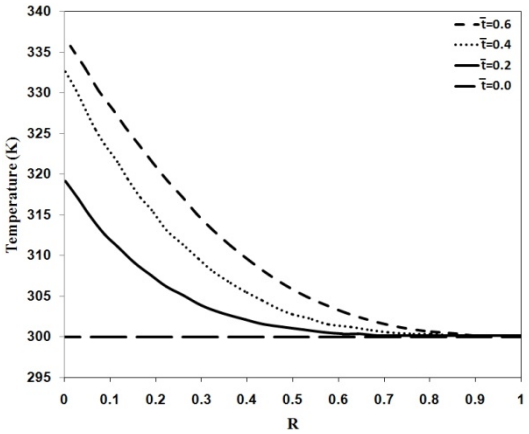

Fig. 3. Temperature distribution vs. dimensionless time for N=1.

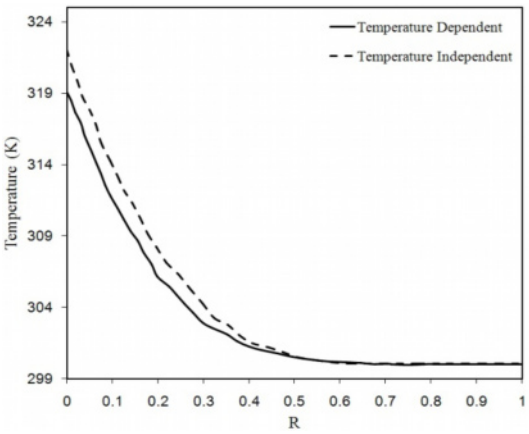

Fig. 6. Temperature distribution for N=1 and $\bar{t} = 0.5$.

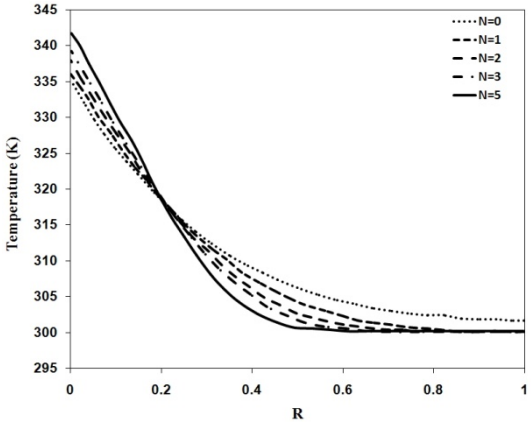

Fig. 4. N effect on temperature distribution for $\bar{t} = 0.5$.

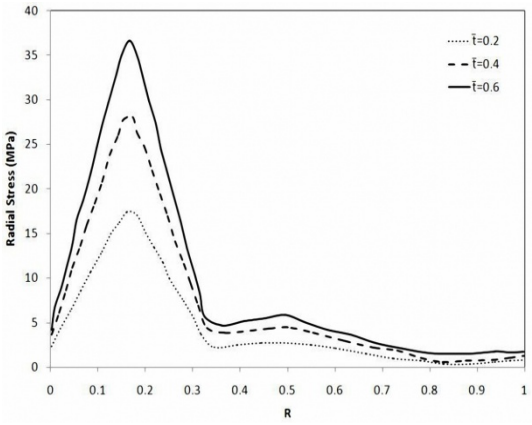

Fig. 7. Radial stress for N=1 versus R and dimensionless time.

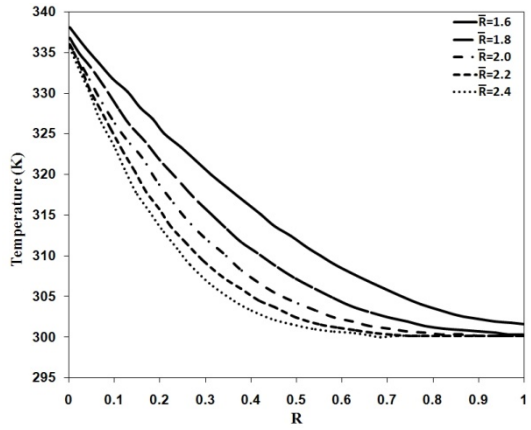

Fig. 5. Geometry effect on temperature distribution for N=1 and $\bar{t} = 0.5$.

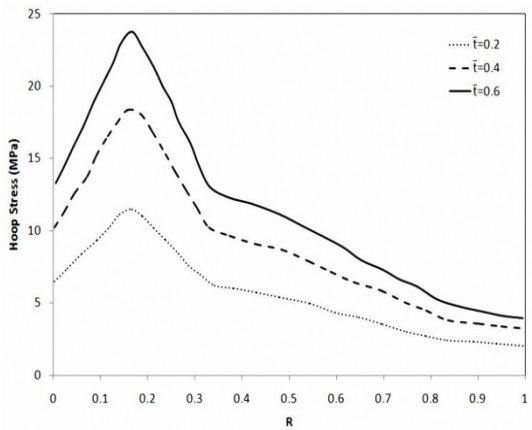

Fig. 8. Hoop stress for N=1 versus R and dimensionless time.

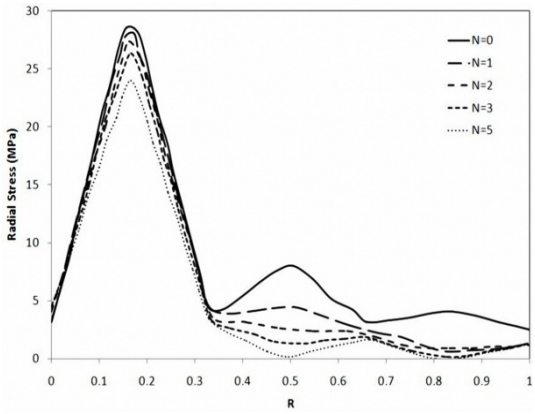

Fig. 9. Radial stress for $\bar{t} = 0.4$ versus R and N.

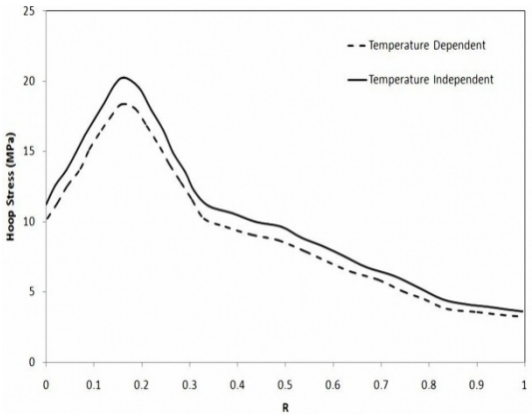

Fig. 12. Hoop stress versus R in $\bar{t} = 0.4$ and N=1.

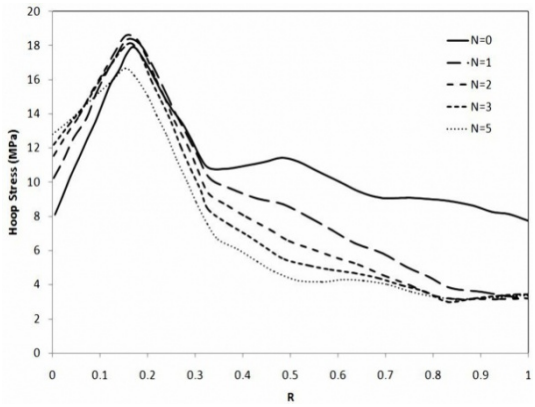

Fig. 10. Hoop Stress for $\bar{t} = 0.4$ versus R and N.

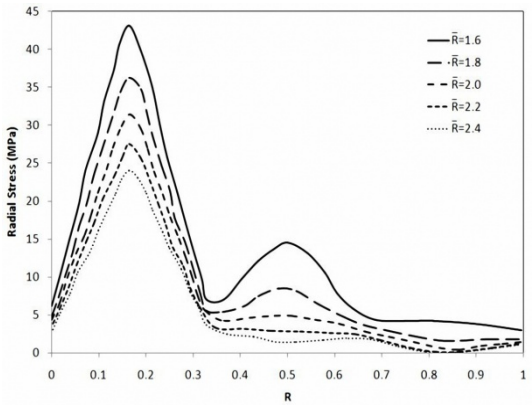

Fig. 13. Geometry effect on radial stress for N=1 and $\bar{t} = 0.4$.

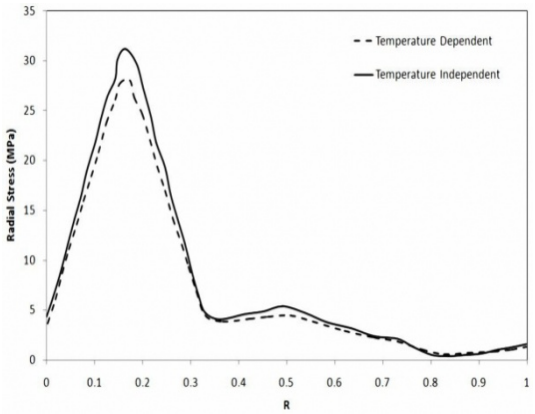

Fig. 11. Radial stress versus R in $\bar{t} = 0.4$ and N=1.

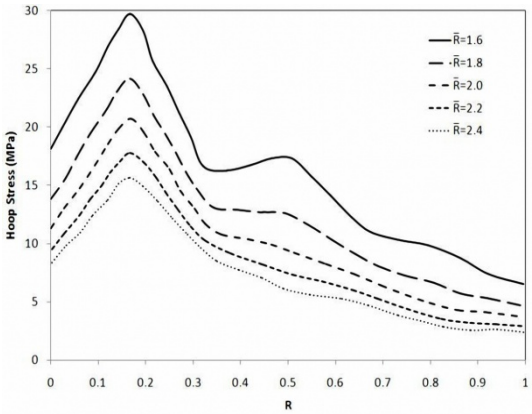

Fig. 14. Geometry effect on hoop stress for N=1 and $\bar{t} = 0.4$.

7. Conclusion

Nonlinear transient heat transfer and thermoelastic analysis of a thick-walled FGM cylinder was analyzed by using a transfinite element method that can be used in an updating and iterative solution scheme. Results also show that the temperature-dependency of the material properties may have significant influence (up to 15 percent) on the temperature distribution and gradient, and also the radial and hoop stresses have a remarkable effect on some critical behaviors such as thermal buckling or dynamic response, crack and wave propagation. Some other parameters such as index of power law (N) and geometrical parameter also have important effects on those mentioned results.

References

[1] N. Noda, Thermal stresses in materials with temperature-dependent properties, *J. Appl. Mech.*, 44 (1991) 83-97.

[2] Y. Tanigawa, Some basic thermoelastic problems for non-homogeneous structural materials, *J. Appl. Mech.*, 48 (1995) 377-389.

[3] M. P. Lutz and R. W. Zimmerman, Thermal stresses and effective thermal expansion coefficient of a functionally graded sphere, *J. Thermal Stresses*, 19 (1996) 39-54.

[4] R. W. Zimmerman and M. P. Lutz, Thermal stress and thermal expansion in a uniformly heated functionally graded cylinder, *J. Thermal Stresses*, 22 (1999) 177-188.

[5] Y. Obata, K. Kanayama, T. Ohji and N. Noda, Two-dimensional unsteady thermal stresses in a partially heated circular cylinder made of functionally graded material, *J. Thermal Stresses*, (1999).

[6] A. Sutradhar, G. H. Paulino and L. J. Gray, Transient heat conduction in homogeneous and non-homogeneous materials by the Laplace transform Galerkin boundary element method, *Eng. Anal. Boundary Element*, 26 (2002) 119-132.

[7] K. S. Kim and N. Noda, Green's function approach to unsteady thermal stresses in an infinite hollow cylinder of functionally graded material, *Acta Mechanics*, 156 (2002) 145-161.

[8] G. N. Praveen and J. N. Reddy, Nonlinear transient thermoelastic analysis of functionally graded ceramic–metal plates, *Int. J. Solids Struct.*, 35 (1998) 4457-4476.

[9] J. N. Reddy and C. D. Chin, Thermomechanical analysis of functionally graded cylinders and plates, *Int. J. Solids Struct.*, 21 (1998) 593-626.

[10] G. N. Praveen, C. D. Chin and J. N. Reddy, Thermoelastic analysis of a functionally graded ceramic–metal cylinder, *ASCE J. Engineering Mech.*, 125 (1999) 1259-1267.

[11] J. N. Reddy, Analysis of functionally graded plates, *Int. J. Numerical Meth. Eng.*, 47 (2000) 663-684.

[12] J. N. Reddy and Z. Q. Cheng, Three-dimensional thermo-mechanical deformations of functionally graded rectangular plates. *Euro. J. Mech. A/Solids*, 20 (2001) 841-860.

[13] J. N. Reddy and Z. Q. Cheng, Frequency of functionally graded plates with three-dimensional asymptotic approach, *J. Engineering Mech.*, 129 (2003) 896-900.

[14] Z. S. Shao, Mechanical and thermal stresses of a functionally graded hollow circular cylinder with finite length, *Int. J. Pressure Vessel Pipe*, 82 (2005) 155-163.

[15] Z. S. Shao and T. J. Wang, Three-dimensional solutions for the stress fields in functionally graded cylindrical panel with finite length and subjected to thermal/mechanical loads, *Int. J. Solids Struct.*, 43 (2006) 3856-3874.

[16] Z. S. Shao, T. J. Wang and K. K. Ang, Transient thermo-mechanical analysis of functionally graded hollow circular cylinders, *J. Thermal Stresses*, 30 (2007) 81-104.

[17] Y. Ootao and Y. Tanigawa, Three-dimensional transient thermal stresses of functionally graded rectangular plate due to partial heating, *J. Thermal Stresses*, 22 (1999) 35-55.

[18] Y. Ootao and Y. Tanigawa, Transient thermoelastic problem of functionally graded thick strip due to non-uniform heat supply, *Composite Struct.*, 63 (2) (2004) 139-146.

[19] Y. Ootao and Y. Tanigawa, Two-dimensional thermoelastic analysis of a functionally graded cylindrical panel due to non-uniform heat supply, *Mech. Res. Commun.*, 32 (2005) 429-443.

[20] K. M. Liew, S. Kitipornchai, X. Z. Zhang and C. W. Lim, Analysis of the thermal stress behavior of functionally graded hollow circular cylinders, *Int. J. Solids Struct.*, 40 (2003) 2355-2380.

[21] H. Awaji and R. Sivakuman, Temperature and stress distributions in a hollow cylinder of functionally graded material: the case of temperature-dependent material properties, *J. Am. Ceram. Soc.*,

84 (2001) 59-1065.

[22] H. K. Ching and S. C. Yen, Transient thermoelastic deformations of 2-D functionally graded beams under non-uniformly convective heat supply, *Composite Struct.*, 73 (4) (2006) 381-393.

[23] G. Honig and U. Hirdes, A method for the numerical inversion of Laplace transforms, *J. Computer Appl. Math.*, 10 (1984) 113-132.

Mohammad Azadi received his B.S. in Mechanical Engineering from Shiraz University, Iran, in 2006. He then received his M.S. degree from K.N. Toosi University of Technology in 2008. Now, he is currently a Ph.D student at Sharif University of Technology. Azadi's research interests include NVH, fatigue, Composites (FGMs), Finite Element Method (FEM) and automotive engineering.